Dentomaxillofacial Radiology (2017) 46, 20160407

birpublications.org/dmfr

TECHNICAL REPORT

"Black Bone" MRI: a novel imaging technique for 3D printing

[1,2]Karen A Eley, [3]Stephen R Watt-Smith and [2,4]Stephen J Golding

[1]*Department of Radiology, Addenbrookes Hospital, Cambridge, UK;* [2]*Nuffield Department of Surgical Sciences, University of Oxford, Oxford, UK;* [3]*Eastman Dental Hospital, UCLH, London, UK;* [4]*University College, University of Oxford, Oxford, UK*

Objectives: Three-dimensionally printed anatomical models are rapidly becoming an integral part of pre-operative planning of complex surgical cases. We have previously reported the "Black Bone" MRI technique as a non-ionizing alternative to CT. Segmentation of bone becomes possible by minimizing soft tissue contrast to enhance the bone–soft tissue boundary. The objectives of this study were to ascertain the potential of utilizing this technique to produce three-dimensional (3D) printed models.
Methods: "Black Bone" MRI acquired from adult volunteers and infants with craniosynostosis were 3D rendered and 3D printed. A custom phantom provided a surrogate marker of accuracy permitting comparison between direct measurements and 3D printed models created by segmenting both CT and "Black Bone" MRI data sets using two different software packages.
Results: "Black Bone" MRI was successfully utilized to produce 3D models of the craniofacial skeleton in both adults and an infant. Measurements of the cube phantom and 3D printed models demonstrated submillimetre discrepancy.
Conclusions: In this novel preliminary study exploring the potential of 3D printing from "Black Bone" MRI data, the feasibility of producing anatomical 3D models has been demonstrated, thus offering a potential non-ionizing alterative to CT for the craniofacial skeleton.
Dentomaxillofacial Radiology (2017) **46**, 20160407. doi: 10.1259/dmfr.20160407

Cite this article as: Eley KA, Watt-Smith SR, Golding SJ. "Black Bone" MRI: a novel imaging technique for 3D printing. *Dentomaxillofac Radiol* 2017; **46**: 20160407.

Keywords: 3D imaging; 3D printing; MRI; segmentation; anatomical models

Introduction

The term rapid prototyping was coined in the 1980s to describe new technologies that produced physical models directly from a three-dimensional (3D) computer-aided design of an object.[1] Within the surgical community, maxillofacial and craniofacial surgeons were among early adopters of this new technology, which soon became routine clinical care.[2–4] The benefits were clear, with physical models providing superior visualization of complex anatomy over both axial and static 3D rendered images, with better surgical planning capabilities and resultant improvements in patient outcomes.[5,6] Evolving advancements in technology saw models produced using computer numerical control milling being gradually replaced by stereolithography and the additive layer processes that are in widespread use today.

Over the past few years, there has been an explosion of interest in 3D printing, fuelled by reduction in associated costs. The range of potential applications is diverse, surpassing surgical planning to include custom-made implantable prostheses and novel teaching and training tools. Today, there are few departments around the world without access to such facilities either in-house or through a commercial company using data transfer *via* the internet.

The fundamental principle underpinning all 3D printing technology in medicine is cross-sectional image acquisition and segmentation, for which radiologists clearly play a vital role. Typically, the imaging modality

Correspondence to: Dr Karen A Eley. E-mail: Karen.a.eley@gmail.com

This study has received funding by AO Foundation (Project no. C-09-01W) & Newlife Foundation for Disabled Children.
Received 12 October 2016; revised 20 January 2017; accepted 24 January 2017

of choice is CT in view of the small voxel size, ease of segmentation and speed of image acquisition. The most simple segmentation technique utilizes thresholding which separates the components of the image according to intensity, aided by the predefined CT numbers (Hounsfield unit) of structures from bone (1000 HU) at one end of the spectrum to air at the other (−1000 HU). Although controversial, concern persists regarding the potential long-term effects of ionizing radiation, particularly when repeated imaging is required in infants and young children. However, whilst MRI offers a non-ionizing alternative, the 3D visualization of complex anatomy is limited. Thresholding-based segmentation is more challenging with MRI since there are no predefined pixel values such as CT, and overlap between adjacent tissues is common. More complex segmentation techniques may be employed such as edge detection, region growing and model-based techniques; however, all these have specific challenges.

We previously reported the potential of an MRI technique that minimizes soft tissue contrast to enhance the bone–soft tissue boundary; hence, the term "Black Bone".[7–11] The novel concept of minimizing soft tissue contrast and any signal returned from bone, rather than using traditional processes to increase signal intensity from bone [*e.g.* ultrashort echo time (TE)], makes it possible to segment bone from the surrounding soft tissues to produce 3D reconstructed images. Early applications of this technique have been particularly promising for the craniofacial skeleton, with results approaching those expected of 3D CT imaging, and in distinguishing normal cranial sutures from those that are prematurely fused (craniosynostosis).[7]

The "Black Bone" MRI technique utilizes a gradient echo (GRE) sequence such as 3D fast GRE (GE Medical Systems Ltd, Chalfont St Giles, UK), volumetric interpolated breath-hold examination (Siemens Healthcare Ltd, Camberley, UK) or an equivalent T_1 weighted GRE 3D volume sequence (Phillips Healthcare, Guildford, UK), with a short TE (4.2 ms)/repetition time (8.6 ms) and a flip angle of 5° with a 1.5- or 3.0-T magnet. The main limitation of the technique arises where air comes into contact with bone, since both return little to no signal, and thus cannot often be reliably distinguished.

The aim of this preliminary study was to explore the potential of producing 3D printed anatomical models from "Black Bone" MRI data sets.

Methods and materials

"Black Bone" MRI data sets utilized for this study were previously acquired from infants and adult volunteers, for which ethical approval had been granted from the Oxfordshire Research Ethics Committee (09/H0606/2).[7] All patient and volunteer imaging used in this study was acquired on a 1.5-T magnet (GE Medical Systems Ltd, Chalfont St Giles, UK; or Phillips Healthcare Ltd, Camberley, UK), with an average acquisition time of 4 min for the craniofacial skeleton.

A custom geometric cube phantom made from poly methyl methacrylate (acrylic) was utilized as a surrogate for dimensional assessment. No prior attempts have ever been made to 3D print from "Black Bone" MRI data, and whilst the phantom was unable to reflect the complexities of the craniofacial skeleton, initial confirmation of the dimensional accuracy was required. The cube phantom permitted direct comparison between 3D models produced from CT and "Black Bone" MRI data, in addition to measurements performed directly on the phantom (gold standard). The cube was sequentially imaged with CT and "Black Bone" MRI with both a 1.5- and 3.0-T magnet (GE Medical Systems Ltd, Chalfont St Giles, UK). The parameters utilized included a 3D fast GRE sequence with a TE of 4.2 ms, repetition time of 8.6 ms, a flip angle of 5°, field of view of 240 mm and matrix size of 512 × 512. To overcome the inherent problem of air in direct contact with the cube, the phantom was imaged submerged in a container of gelatine.

All digital imaging and communications in medicine data were imported into both Mimics v. 14.01 (Materialise, Leuven, Belgium) and Osirix v. 4.1.2 (Open Source), and adapted thresholding techniques were used to segment the 3D data sets. In Osirix, this involved creating a region of interest (ROI) around the soft tissue/gelatine edge and setting the pixel values outside this ROI to a value that no longer coincided with bone. An upper and lower threshold value was set to segment the bone. To standardize the results, a smooth factor of 30 was used in Osirix for all of the cube data sets. In Mimics, a "mask" was created by thresholding the bone. The mask was cropped to remove as much external air as possible and was edited using the "multiple slice edit" function and "edit mask in 3D."

A stereolithographic (STL) file was created and imported into ZPrint 7.6 software (3D Systems, Rock Hill, SC) to communicate with the 3D printer. 3D printing was completed with a Z-Printer 650 printer (3D Systems, Rock Hill, SC), which utilizes an additive layer process, adding binder to a powder layer by layer to gradually build the model. The excess powder was removed by dusting with a brush, and with the aid of a fine high-powered jet of air, and the model coated in cyanoacrylate (standard finishing processes for this technology).

The distances which could be optimally measured on the cube using Vernier callipers were selected, and each distance measured 10 times on the acrylic cube and resultant 3D printed models. As demonstrated in Figure 1, each side of the cube phantom from edge to edge and the diameter of the hole at the top of the cube was measured. As the phantom was custom-made, comparisons of all surfaces were made rather than making the assumption that the sides of the cube were dimensionally equal. Data were entered into Microsoft

Excel, and analysis was performed using SPSS® v. 18.0 Statistical Package for the Social Sciences (IBM Corp., New York, NY; formerly SPSS Inc., Chicago, IL). Comparisons were made between the phantom and the CT and "Black Bone" produced models, using independent samples *t*-test. The discrepancy between the two measurement sets was calculated.

The initial technical feasibility of producing anatomical models from "Black Bone" MRI was explored using an adult volunteer "Black Bone" data set. The mandible was selected in view of the relative simplicity in 3D rendering this region and its comparatively small size. The mandible was segmented in Mimics by applying a threshold and manually removing regions outside of the ROI using the 3D edit functions. An STL file was created from the surface of the 3D rendered image and was subsequently 3D printed.

Results

The first ever produced 3D printed "Black Bone" MRI model of an adult mandible is shown in Figure 2. Following the success of the mandible pilot, a 3D printed model of the entire craniofacial skeleton was produced from a further Black Bone MRI data set (Figure 3). No technical problems were encountered in 3D printing these models.

The final anatomical model printed in this preliminary feasibility study was from an infant with unicoronal synostosis (Figure 4). This model had some technical difficulties in the production stage in view of the particularly thin bone of the facial skeleton and skull base. Since the model was printed on its side, there was some difficulty in removing the contained excess powder, and as a result the skull base broke owing to this added weight when removing the model from the build chamber.

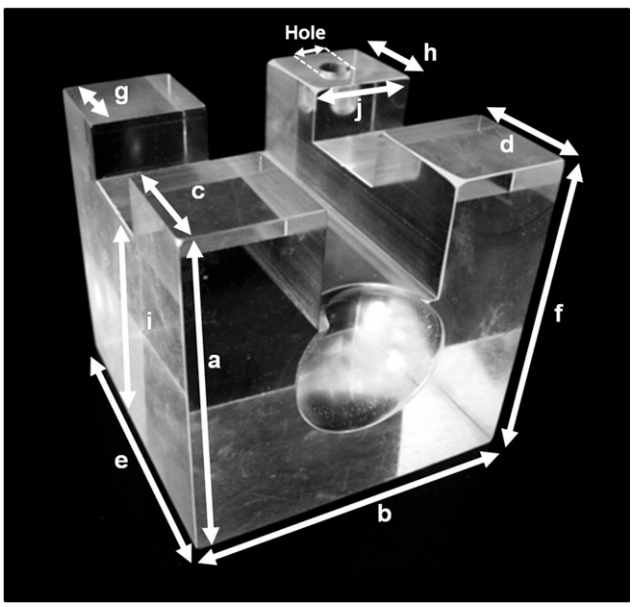

Figure 1 Photograph of the custom-made acrylic cube phantom: this demonstrates the 11 measurements (labelled a–j and hole) which were completed on both the phantom cube and all resultant three-dimensional printed models.

All 3D printed models of the phantom cube from both "Black Bone" MRI and CT data sets rendered with both Osirix and Mimics were produced without complication.

With regard to the 3D printed cube created from CT data, independent samples *t*-test identified a significant difference ($p < 0.05$) between the phantom and the 3D model produced using Mimics for all distances, and for all but two distances for the Osirix model. The mean discrepancy between the model and the phantom using Mimics was 0.86 ± 0.19 mm and 0.36 ± 0.32 mm for Osirix.

The mean ± standard deviation difference between the cube phantom and 3D models produced from both CT and "Black Bone" MRI data sets using Mimics and Osirix is shown in Table 1.

Independent samples *t*-test identified a significant difference between the phantom and the model produced with: (1) 1.5-T data set on Mimics for all distances; (2) 1.5-T data set on Osirix for all but three distances; (3) 3.0-T data set with Mimics for all distances; and (4) 3.0-T data set with Osirix for all but three distances. However, the standard deviation was <0.2 mm for all measurements. The mean discrepancy between the phantom and 3D model was 0.32 ± 0.19 mm for the 1.5-T data set on Mimics, 0.17 ± 0.11 mm for the 1.5-T data set on Osirix, 0.49 ± 0.30 mm for the 3.0-T data set on Mimics and 0.33 ± 0.24 mm for the 3.0-T data set on Osirix.

Overall, the 3D printed models produced from "Black Bone" MRI data sets demonstrated reduced discrepancy from the phantom cube measurements than those produced from CT data rendered with Mimics.

Discussion

We have demonstrated the novel feasibility of 3D printing from "Black Bone" MRI data sets. To our knowledge, this is the first time that 3D printing has ever been successfully achieved from bone segmented on MRI data. "Black Bone" MRI therefore potentially fulfils the full range of image manipulation that craniomaxillofacial surgeons have come to expect from radiology, including orthogonal views, 3D reconstructed imaging and physical models. The potential ability to plan craniofacial surgical intervention in this way not only provides a non-ionizing alternative to CT in the younger more radiosensitive population, but may also reduce the need for multimodality imaging in a wider patient group.

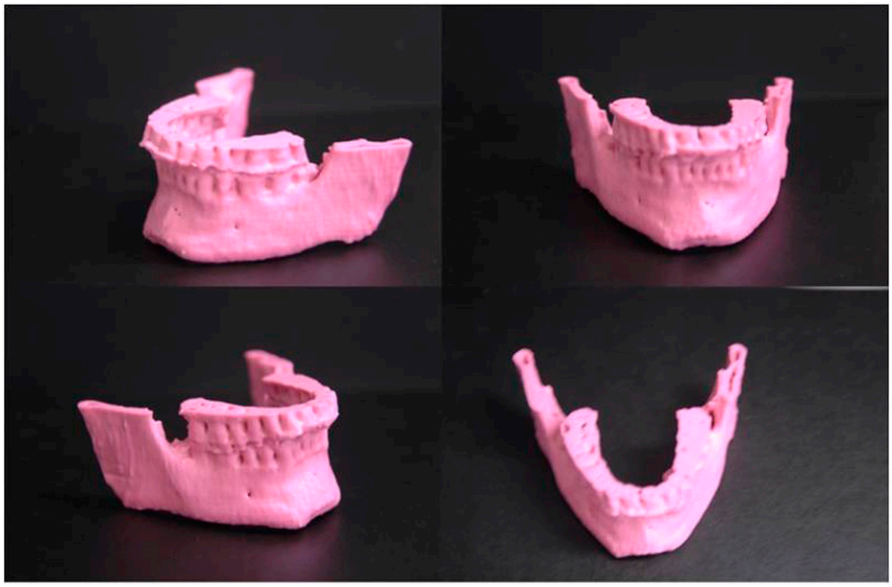

Figure 2 The first three-dimensional printed anatomical model ever produced from "Black Bone" MRI of the mandible of an adult volunteer.

Good-quality 3D printed models can be achieved only if the cross-sectional imaging is also of high quality.[12] Ideally, thin slice thickness and isotropic voxels are desired. Acquiring "Black Bone" MRI data sets as a 3D volume is thus advantageous, but even as a relatively rapid GRE acquisition technique, "Black Bone" MRI cannot compete with the speed of CT imaging. The typical acquisition time for the craniofacial skeleton is 4 min compared with a matter of seconds for CT. As a result, there is increased risk of movement artefact, and potential reliance upon sedation or general anaesthesia in young children. However, in those patients already undergoing MRI, acquisition of "Black Bone" MRI adds only a small amount of time to the overall examination and may ultimately negate the requirement for CT. "Black Bone" MRI is susceptible to the same artefact as any standard GRE sequence. Within the craniofacial skeleton, this is most problematic when there is significant metal work, such as fixed orthodontic appliances. However, the artefact seen with dental amalgam for example is significantly lesser than the streak artefact seen on CT.

Having acquired good-quality imaging, the next step in the process is image manipulation and segmentation, invariably the most time-intensive step in producing anatomical models. Whilst this is a relatively straightforward process when pixel values of adjacent tissues do not overlap or where there is a distinct boundary, this is rarely the case with MRI. Success has previously been reported with MRI for some soft tissue structures such

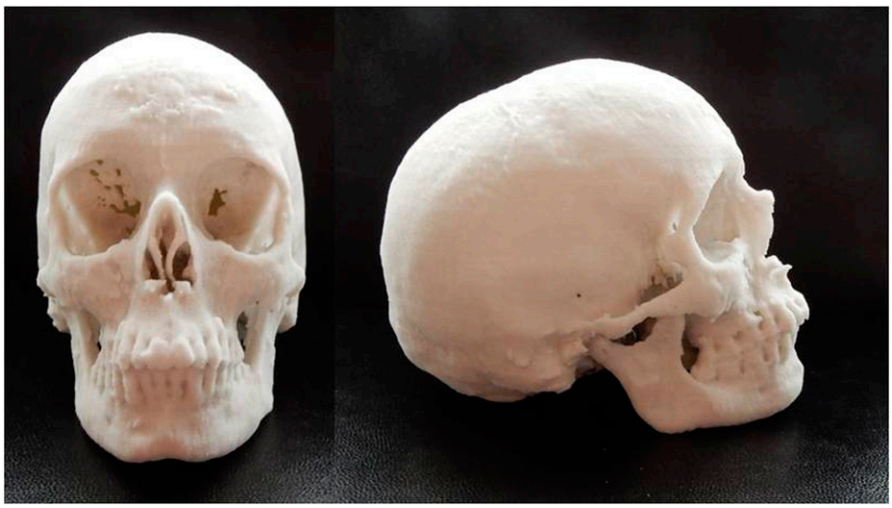

Figure 3 A three-dimensional printed model of the craniofacial skeleton of an adult volunteer from "Black Bone" MRI data.

Figure 4 Frontal and superior views of a three-dimensional (3D) printed anatomical model from "Black Bone" MRI data set of an infant with unicoronal synostosis: the technical limitations of the 3D printing technology and thin bone resulted in some regions of inaccuracy within the facial skeleton.

as the heart and brain;[13–15] however, CT remains the imaging modality of choice in the majority of 3D printing examples in the literature. Whilst "Black Bone" MRI goes some way to address the problem by enhancing the soft tissue–bone boundary, at present it is not a perfect solution. Both Mimics and Osirix used in this study are largely reliant upon thresholding-based segmentation, which requires manual adjustment in areas where there is overlap in pixel values, and were more challenging in infants owing to the thin cranial bone. We have previously worked with volume rendering software such as High Definition Volume Rendering® software by Fovia, Inc. (Palo Alto, CA), which provide superior 3D rendered images with reduction in the time required for image manipulation; however, at the time of this study, an STL export function was not available.

As previously discussed, both air and bone result in signal void on "Black Bone" MRI, resulting in inherent difficulties whenever these come into direct contact. This is seen on the model of the mandible where the upper incisors were incompletely covered by soft tissues, and these teeth required manual separation from air. Whilst this can be potentially overcome by simply asking the patient to maintain an adequate lip seal, areas such as bone abutting the air sinuses or the external ear canal are particularly problematic. This problem was addressed by imaging the phantom cube submerged in gelatine, an option clearly not possible when imaging patients.

A statistically significant difference was seen between the measurements completed on the cube phantom and the 3D printed models produced both from CT and MRI data sets. This was deemed to be the result of a combination of factors. The cube phantom is not perfectly uniform in size to the degree with which it was being measured (0.01 mm), meaning that error may have been introduced simply by selecting a site marginally higher or lower than the previous measurements. Being made of acrylic (cube phantom) or plaster/binder (3D model), it is possible that some variation was introduced as a result of the tightness with which the Vernier callipers were opposed owing to variability in the mechanical properties of each measured object. However, the discrepancy in measurements between the phantom cube and the 3D printed models was <1 mm. Whilst the cube phantom does not by any means provide an accurate representation of the complexities of the craniofacial skeleton, if comparable results were achieved in patients, this would correlate to a level of discrepancy unlikely to be of clinical relevance. These findings in the cube phantom are particularly

Table 1 Mean ± standard deviation direct measurement of the cube phantom, and the difference between Phantom and model using CT and "Black Bone (BB)" data sets on Mimics (Materialise, Leuven, Belgium) and Osirix

Cube Measurement	*Direct phantom measurement (mm)*	*CT Mimics*	*CT Osirix*	*BB 1.5 T Mimics*	*BB 1.5 T Osirix*	*BB 3.0 T Mimics*	*BB 3.0 T Osirix*
A	60.11 ± 0.03	0.96 ± 0.08	0.85 ± 0.04	0.07 ± 0.03	0.10 ± 0.05	0.82 ± 0.12	0.30 ± 0.09
B	60.09 ± 0.02	0.73 ± 0.07	0.47 ± 0.15	0.13 ± 0.07	0.26 ± 0.07	0.14 ± 0.02	0.08 ± 0.06
C	20.07 ± 0.03	0.82 ± 0.05	0.17 ± 0.08	0.34 ± 0.05	0.24 ± 0.15	0.42 ± 0.07	0.41 ± 0.04
D	20.08 ± 0.03	0.76 ± 0.04	0.07 ± 0.07	0.24 ± 0.08	0.26 ± 0.07	0.59 ± 0.05	0.31 ± 0.04
E	60.11 ± 0.03	0.86 ± 0.04	0.03 ± 0.02	0.66 ± 0.06	0.17 ± 0.07	0.14 ± 0.05	0.73 ± 0.15
F	60.18 ± 0.25	0.94 ± 0.09	0.69 ± 0.04	0.07 ± 0.05	0.04 ± 0.05	0.89 ± 0.10	0.27 ± 0.08
G	19.88 ± 0.03	0.73 ± 0.03	0.13 ± 0.08	0.42 ± 0.08	0.11 ± 0.11	0.30 ± 0.04	0.55 ± 0.04
H	19.91 ± 0.03	0.71 ± 0.03	0.17 ± 0.05	0.30 ± 0.07	0.18 ± 0.09	0.34 ± 0.08	0.68 ± 0.05
I	49.89 ± 0.03	1.18 ± 0.18	0.91 ± 0.15	0.29 ± 0.13	0.1 ± 0.07	0.70 ± 0.04	0.11 ± 0.08
J	19.99 ± 0.02	0.65 ± 0.03	0.13 ± 0.02	0.46 ± 0.02	0.26 ± 0.02	0.16 ± 0.03	0.02 ± 0.03
Hole	5.84 ± 0.04	1.16 ± 0.16	0.29 ± 0.21	0.50 ± 0.13	0.15 ± 0.08	0.92 ± 0.07	0.20 ± 0.12

reassuring when consideration is given to the multiple steps where error can arise, including segmentation, the software package and segmentation tools used, any smoothing factors applied and the printing process itself. Visually, these early attempts at 3D printing of the craniofacial skeleton from "Black Bone" MRI are very encouraging, and the results obtained from the adult volunteer approach those for CT data from this type of 3D printing technology. Difficulties were encountered with the model produced from an infant with craniosynostosis, owing to a combination of the thin bone encountered at this age and the limitations of the particular 3D printing technology used in this study, problems that can be encountered irrespective of the imaging modality from which the data set was obtained. These difficulties could be overcome most simply by utilizing 3D printing technologies that do not rely on powder as a support structure in cases where the bone is particularly thin.

Whilst the dimensional accuracy was confirmed with a cube phantom, further investigation is required with direct comparison between CT and "Black Bone" MRI of the craniofacial skeleton. This is particularly of interest in regions where air and bone come into close contact resulting in difficulties with segmentation. Whether clinicians are prepared to accept these potential discrepancies in return for a radiation-free technique for their patients remains to be seen.

The segmentation techniques used for "Black Bone" MRI are currently user dependent and as a result may be labour intensive for the inexperienced. We continue to further adapt our image segmentation techniques, aiming for a fully automated process that will bring the time required for image manipulation more in line with that currently achieved with CT. Our ongoing research utilizes a range of both commercial and open source software. We also actively seek collaborators to help take this work forward.

In conclusion, this preliminary feasibility study has demonstrated that "Black Bone" MRI offers a potential alternative to CT in the production of anatomical models. Further confirmation of the accuracy of the techniques is required in addition to the successful development of automated "Black Bone" MRI segmentation techniques required to permit incorporation into routine clinical practice in the future.

Acknowledgments

The work was completed at the Nuffield Department of Surgical Sciences, University of Oxford.

References

1. Bibb R. Pre-operative management—modelling and rapid prototyping. *Imaging and planning in surgery: a guide to research*. Switzerland: AO Publishing; 2008.
2. Eley KA, Richards R, Dobson D, Linney A, Watt-Smith SR. Re.: Development of in-house rapid manufacturing of three-dimensional models in maxillofacial surgery. *Br J Oral Maxillofac Surg* 2011; **49**: 326–7. doi: https://doi.org/10.1016/j.bjoms.2010.09.019
3. Lill W, Solar P, Ulm C, Watzek G, Blahout R, Matejka M. Reproducibility of three-dimensional CT-assisted model production in the maxillofacial area. *Br J Oral Maxillofac Surg* 1992; **30**: 233–6. doi: https://doi.org/10.1016/0266-4356(92)90265-K
4. Sailer HF, Haers PE, Zollikofer CP, Warnke T, Carls FR, Stucki P. The value of stereolithographic models for preoperative diagnosis of craniofacial deformities and planning of surgical corrections. *Int J Oral Maxillofac Surg* 1998; **27**: 327–33. doi: https://doi.org/10.1016/S0901-5027(98)80059-3
5. Imai K, Tsujiguchi K, Toda C, Enoki E, Sung KC, Sakamoto H, et al. Reduction of operating time and blood transfusion for craniosynostosis by simulated surgery using three-dimensional solid models. *Neurol Med Chir (Tokyo)* 1999; **39**: 423–6; discussion 427. doi: https://doi.org/10.2176/nmc.39.423
6. Erickson DM, Chance D, Schmitt S, Mathis J. An opinion survey of reported benefits from the use of stereolithographic models. *J Oral Maxillofac Surg* 1999; **57**: 1040–3. doi: https://doi.org/10.1016/S0278-2391(99)90322-1
7. Eley KA, Watt-Smith SR, Sheerin F, Golding SJ. "Black Bone" MRI: a potential alternative to CT with three-dimensional reconstruction of the craniofacial skeleton in the diagnosis of craniosynostosis. *Eur Radiol* 2014; **24**: 2417–26. doi: https://doi.org/10.1007/s00330-014-3286-7
8. Eley KA, Watt-Smith SR, Golding SJ. "Black bone" MRI: a potential alternative to CT when imaging the head and neck: report of eight clinical cases and review of the Oxford experience. *Br J Radiol* 2012; **85**: 1457–64. doi: https://doi.org/10.1259/bjr/16830245
9. Eley KA, McIntyre AG, Watt-Smith SR, Golding SJ. "Black bone" MRI: a partial flip angle technique for radiation reduction in craniofacial imaging. *Br J Radiol* 2012; **85**: 272–8. doi: https://doi.org/10.1259/bjr/95110289
10. Eley KA, Watt-Smith SR, Golding SJ. "Black Bone" MRI: a potential non-ionizing method for three-dimensional cephalometric analysis—a preliminary feasibility study. *Dentomaxillofac Radiol* 2013; **42**: 20130236. doi: https://doi.org/10.1259/dmfr.20130236
11. Eley KA, Watt-Smith SR, Golding SJ. Three-Dimensional Reconstruction of the Craniofacial Skeleton With Gradient Echo Magnetic Resonance Imaging ("Black Bone"): What Is Currently Possible? *J Craniofac Surg* 2017; Jan 20. doi: https://doi.org/10.1097/SCS.0000000000003219. [Epub ahead of print]
12. Rengier F, Mehndiratta A, von Tengg-Kobligk H, Zechmann CM, Unterhinninghofen R, Kauczor HU, et al. 3D printing based on imaging data: review of medical applications. *Int J Comput Assist Radiol Surg* 2010; **5**: 335–41. doi: https://doi.org/10.1007/s11548-010-0476-x
13. Byrne N, Velasco Forte M, Tandon A, Valverde I, Hussain T. A systematic review of image segmentation methodology, used in the additive manufacture of patient-specific 3D printed models of the cardiovascular system. *JRSM Cardiovasc Dis* 2016; **5**: 2048004016645467. doi: https://doi.org/10.1177/2048004016645467
14. Biglino G, Capelli C, Wray J, Schievano S, Leaver LK, Khambadkone S, et al. 3D-manufactured patient-specific models of congenital heart defects for communication in clinical practice: feasibility and acceptability. *BMJ Open* 2015; **5**: e007165. doi: https://doi.org/10.1136/bmjopen-2014-007165
15. Spottiswoode BS, van den Heever DJ, Chang Y, Engelhardt S, Du Plessis S, Nicolls F, et al. Preoperative three-dimensional model creation of magnetic resonance brain images as a tool to assist neurosurgical planning. *Stereotact Funct Neurosurg* 2013; **91**: 162–9. doi: https://doi.org/10.1159/000345264